Synthesis and Characterization of Benzo[1,2-b:3,4-b′:5,6-b″]trithiophene (BTT) Oligomers

Tomoya Kashiki,[†] Masahiro Kohara,[†] Itaru Osaka,[†] Eigo Miyazaki,[†] and Kazuo Takimiya*,[†,‡]

[†]Department of Applied Chemistry, Graduate School of Engineering, Hiroshima University, Higashi-Hiroshima 739-8527, Japan
[‡]Institute for Advanced Materials Research, Hiroshima University, Higashi-Hiroshima 739-8530, Japan

S *Supporting Information*

ABSTRACT: Two dimers (**2** and **3**), dendritic tetramer (**4**), hexamer (**5**), and decamer (**6**) of benzo[1,2-b:3,4-b′:5,6-b″]trithiophene (BTT), a potential π-core unit with C_{3h} symmetry, were synthesized, characterized, and evaluated for possible use as organic semiconductors. Single crystal X-ray analyses of the dimers (**2** and **3**) revealed that they have planar molecular structures with dihedral angles of almost 180° between two BTT units. In accordance with the rigid and planar molecular structure, the unsubstituted dimer (**2**) is poorly soluble, whereas the octyl-substituted dimer (**3**) has improved solubility. Although the solubility of the dendritic tetramer (**4**) is decreased, further extended systems, i.e., the dendritic hexamer (**5**) and decamer (**6**), have solubilities better than that of **4**. With increasing numbers of BTT units in the molecule, the experimentally determined energy levels of HOMO shift upward slightly and the HOMO−LUMO energy gaps become smaller, but the extent of HOMO destabilization and reduction of the HOMO−LUMO gap are not significant. Taking into account the energy levels of the frontier orbitals, **3**−**6** could be useful as p-channel organic semiconductors rather than n-channel. In fact, the spin-coated thin film of **3** with edge-on molecular orientation acted as an active channel of field-effect transistors that showed hole mobilities as high as 0.14 cm^2 V^{-1} s^{-1}, indicating that the BTT core is a useful π-conjugated system for application to organic semiconductors, although **4**−**6** gave FET characteristics rather inferior to those of **3**, owing to their amorphous nature in the thin film state.
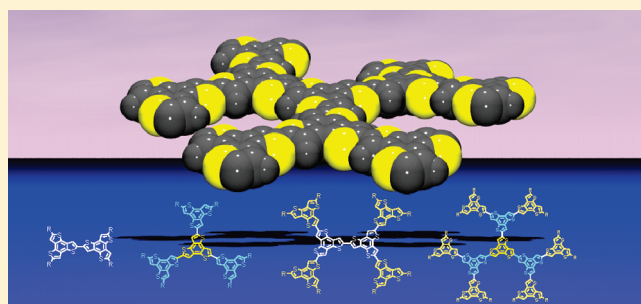
■ INTRODUCTION

Recent prevailing interest in organic electronics has prompted synthetic chemists to innovate new π-conjugated molecules that are applicable to electronic materials.[1] Representative molecular classes used as electronic materials include oligoacenes,[2] oligo- and polythiophenes,[3] phthalocyanines,[4] hexabenzocoronenes,[5] and heteroarenes.[6] These π-conjugated molecules and polymers, often referred to as organic semiconductors, have been widely utilized in various opto/electronic applications, such as organic light-emitting diodes (OLEDs), organic field-effect transistors (OFETs), and organic photovoltaics (OPVs). For the further development of new molecular classes, the rational design of molecular electronic structures is a key. In addition, the shape of a molecule also plays a crucial role in the electronic applications, because molecular ordering in the solid state, mainly the thin film state, governs intermolecular orbital overlaps and hence carrier transport properties. Given these circumstances, we have focused on benzo[1,2-b:3,4-b′:5,6-b″]trithiophene[7] (BTT **1a**, Figure 1) as a potential π-core for a new class of organic semiconductors for the following reasons. First, its planar and rigid π-framework can promote strong intermolecular interaction that would be suitable for developing organic semiconducting materials. Second, the BTT core is a rare structure having three identical

thiophene moieties with C_{3h} symmetry that enables two-dimensional (2D) molecular extension and even more dendritic three-dimensional (3D) extension with star-shaped structures, provided that multiple BTT oligomerization is possible. In fact, such star-shaped π-conjugated oligomers have attracted recent attention as new types of organic semiconducting materials with multiple π-conjugate units with monodisperse, well-defined, discrete molecular structures.[8]

Despite its unique molecular structure and potential use as a building block for organic semiconductors, the application of the BTT core remains severely limited. To our knowledge, only several application in the field of materials chemistry have been reported, e. g., oligothiophene-substituted derivatives (**1b**) that have been utilized as p-channel organic semiconductors for OPVs,[9] the core unit for cross-linked polymer with ethylenedioxythiophene (ED-OT) units,[10] and the core structure for the hexagonal columnar mesogen (**1c**) with moderately high mobility.[11] Simple BTT oligomers, even the dimer of BTT, have yet to be synthesized. In this article, we report the synthesis and characterization of BTT dimers (**2**, **3**), dendritic tetramer (**4**), hexamer (**5**), and decamer
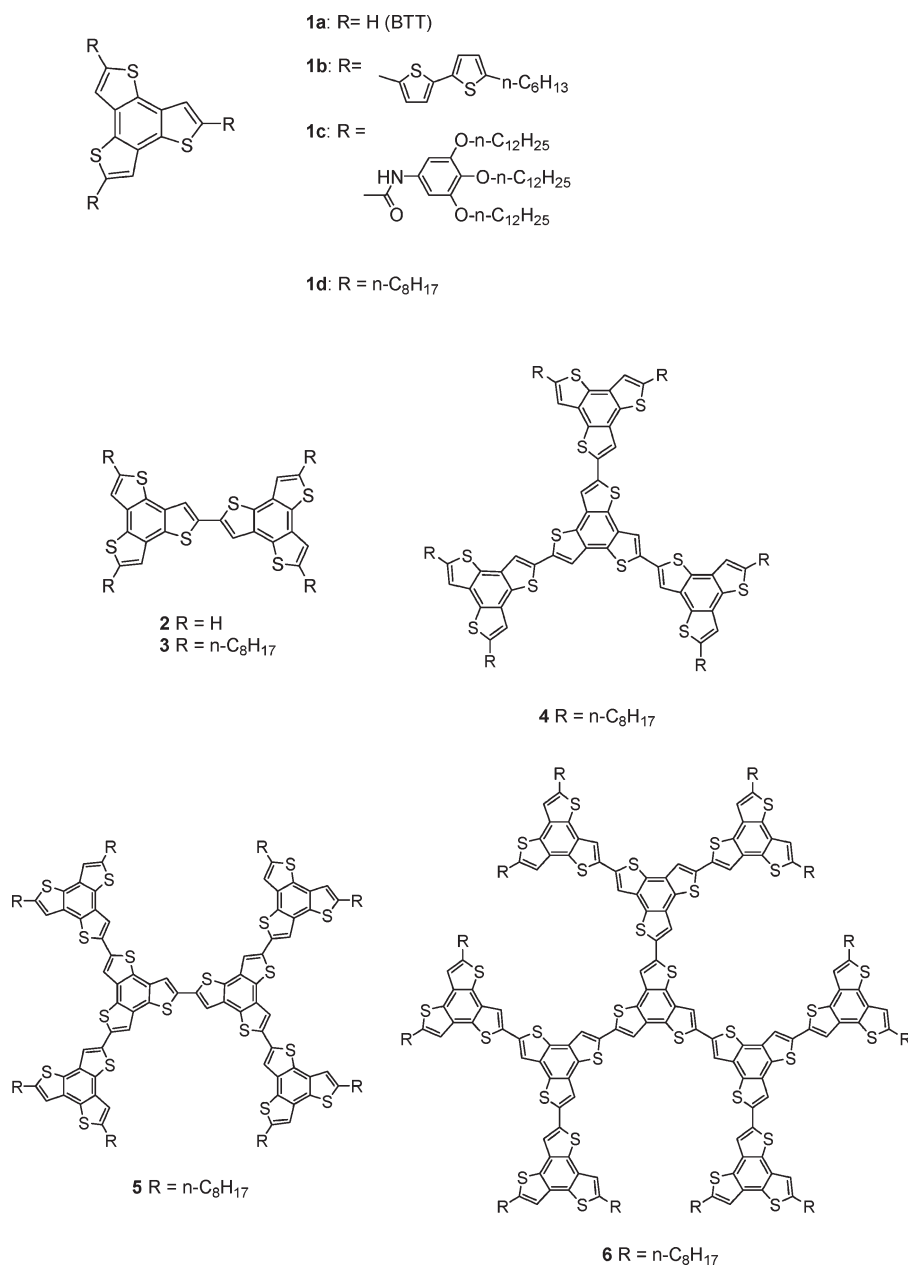
Figure 1. Structures of BTT and its oligomers.

(6) together with fabrication and characterization of their thin films. We also examined their use as the active semiconducting material in organic field-effect transistors (OFETs) and found that the dimer (3) capable of affording well-ordered thin film by solution deposition gave decent OFETs with mobility up to 0.14 cm^2 V^{-1} s^{-1}.

■ RESULTS AND DISCUSSION

Synthesis. Although the first synthesis of the parent BTT (1a) dates back to the early work of Proetzsch et al. in 1972,[7] the tediousness of the synthesis has hindered various derivatizations of it. However, thanks to the recently established straightforward procedure for the synthesis of 1a,[10,12] it is now available in multigram scale in our laboratory. Thus, using 1a as the starting material, we first synthesized the dimer of BTT (2) via direct

monolithiation followed by oxidative coupling effected by Fe-(acac)$_3$ in 61% isolated yield (Scheme 1). The structure of 2 was confirmed by mass spectrometry, combustion analysis, and single-crystal X-ray analysis (Figure 2a). Similar to conventional thiophene—thiophene junctions in oligothiophenes,[3] 2 has a planar structure with a dihedral angle of 180°. In the crystal lattice the molecules of 2 pack tightly in the π-stacking columnar structure with a separation of 3.54 Å (Figure 2b). Because of its rigid and planar molecular structure as well as the tight packing in the crystal structure, 2 is poorly soluble in a range of organic solvents, implying difficulty of the synthesis of higher BTT oligomers than the dimer. To circumvent this problem, we introduced two n-octyl groups to the BTT core for solubilization to furnish dioctyl-BTT (7), and then 7 was similarly dimerized to tetraoctyl dimer (3), which turned out to be fairly soluble (solubility = 1.7 g L^{-1} in chloroform at rt). We also confirmed

the molecular structure of **3** by means of single crystal X-ray analysis; as in the case for the unsubstituted **2**, **3** has a similar planar molecular structure with a dihedral angle of almost 180° at the junction between two BTT units (Figure 3a), indicating that the octyl groups introduced do not hinder effective conjugation between the BTT units. In addition, intermolecular π-stacking structure is preserved in the crystal of **3**, although there exists the slippage of molecules along both the molecular short and long axes directions (Figure 3b). From these structural aspects of **3** both at the molecular and intermolecular level, we concluded that **7** is a useful building block for further oligomerization with keeping good coplanarity, $\pi-\pi$ intermolecular interaction, and sufficient solubility.

Using the soluble BTT monomer (**7**), we then synthesized the dendritic oligomers (**4−6**) as depicted in Scheme 2. Monomer **7** was first converted into trimethylstannyl derivative (**8**), which
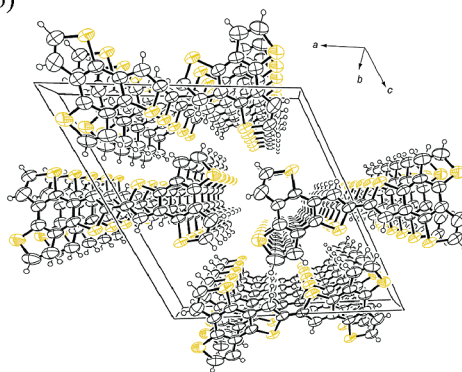
Scheme 1. Synthesis of BTT Dimers (2 and 3)
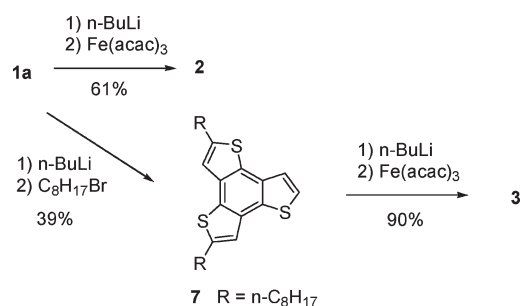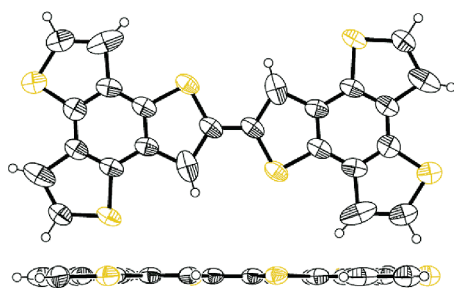
was subsequently coupled in the presence of palladium catalyst with tribromo-BTT (**9**), prepared by reacting **1a** with *N*-bromosuccinimide in moderate yield, to give the tetramer (**4**) in 81% yield after purification. For further derivatization, a trimeric dendron unit with a bromine moiety (**10**) was readily prepared via the palladium-catalyzed Stille coupling between **9** and 2-fold **8** in a moderate yield (42%). In contrast, the synthesis of a trimeric dendron with a trimethylstannyl group (**13**) was somehow troublesome. Thus, after examination of several possible synthetic routes, including a conversion of **10** to **13** via lithium−bromine exchange reaction followed by a reaction with trimethyltin chloride, we finally found an efficient synthetic route to **13** via the Stille coupling between tris(trimethylstannyl)BTT (**11**) and dioctyl-iodo-BTT (**12**) (Scheme 2). With these trimeric dendrons possessing the reacting substituents, the hexamer (**5**) was easily obtained via the simple 1:1 Stille coupling between **10** and **13** (67% isolated yield).

The dendritic decamer (**6**) could be synthesized via the Stille cross-coupling reaction between **10** and **11** or **9** and **13**. We tested both combinations and found that the latter gave the desired decamer (**6**) in 33% isolated yield. In sharp contrast, the former gave a complex mixture consisting of various polymers judged from its MALDI-TOF mass spectra. This can be explained by the concomitant reductive self-coupling reaction of **11** at the trimethylstannyl site, which competes with the desired cross-coupling under the reaction conditions, giving a random mixture of BTT oligomers with multiple trimethylstannyl substituents that further react to produce a mixture of various BTT
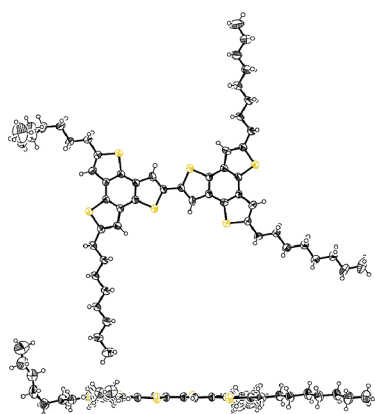
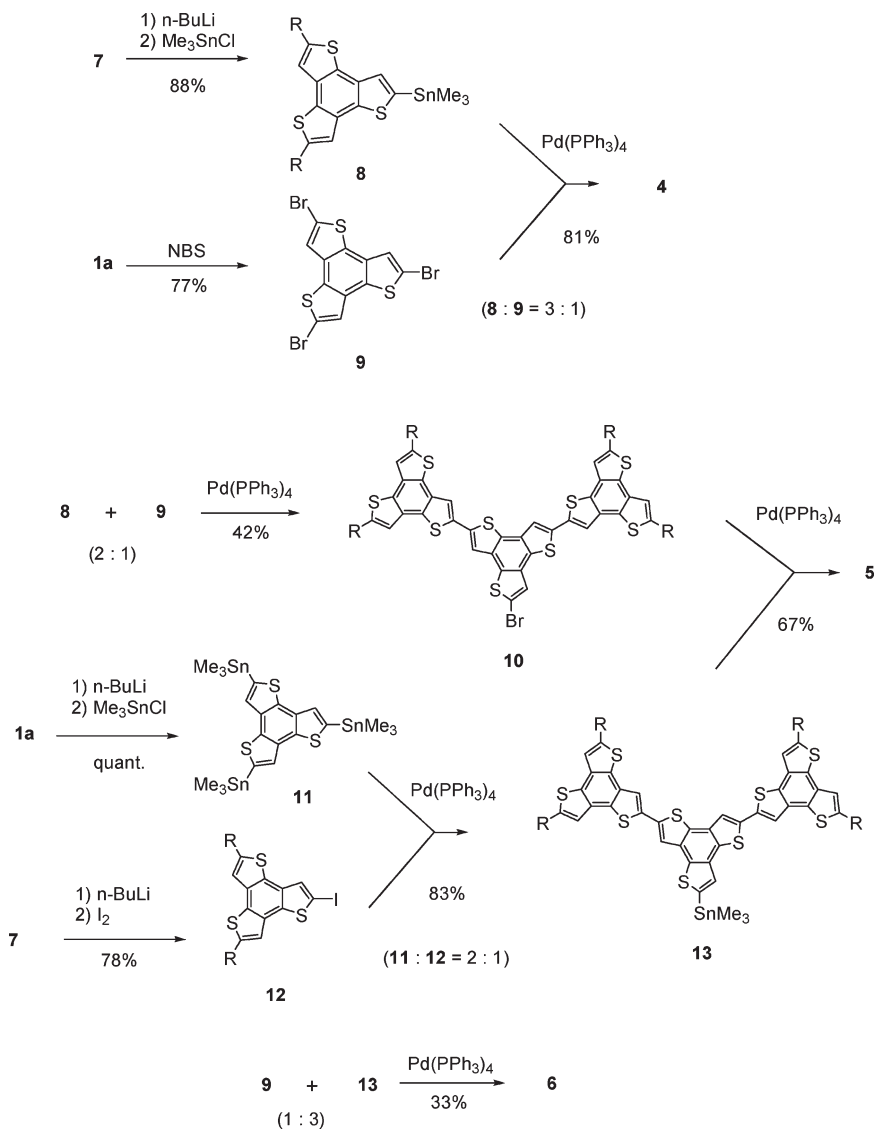**Figure 2.** Molecular structure (a) and crystal structure of **2** (b).

Figure 3. Molecular structure (a) and stacking structure of **3** (b).

Scheme 2. Synthesis of BTT Tetramer (4), Hexamer (5), and Decamer (6)

oligomers and polymers. In fact, the latter combination also gave the hexamer (**5**) as a byproduct, which is supposed to be formed via the reductive self-coupling of **13**.

It is interesting to note that the solubilities of **5** (5.3 g L^{-1} in chloroform at rt) and **6** (6.4 g L^{-1}) are fairly improved, compared to that of **3** (1.7 g L^{-1}) and **4** (0.2 g L^{-1}). This can be partially explained by the fact that the large oligomers have a larger numbers of solublizing octyl side groups. However, relative numbers the octyl groups to the BTT core are reducing with increasing the size of oligomers: two octyl groups per BTT unit for **3**, 1.5 for **4**, 1.33 for **5**, and 1.2 for **6**. Thus, not only the numbers of octyl groups but also the planarity of the molecules must play an important role for the solubility. In fact, the molecules of **3** and **4** that can have planar molecular geometries enables effective intermolecular π—stacking interaction, reducing solubility. On the other hand, the larger oligomers **5** and **6** cannot assume a coplanar structure for all the BTT units because of the steric bulk caused by the peripheral octyl groups. This steric effect is much pronounced in **6**, which well explains the highest solubility of **6** among the present oligomers.

Molecular Properties. As mentioned above alkylated dimer (**3**), tetramer (**4**), hexmaer (**5**), and decamer (**6**) are sufficiently soluble for evaluation of their molecular electronic properties by means of solution electrochemistry and optical spectroscopy. Cyclic voltammograms of **3**—**6** showed oxidation processes with oxidation onsets at +0.72—0.92 V (vs Ag/AgCl), which corresponded to the HOMO energy levels (E_{HOMO}) of ca. 5.0—5.3 eV below the vacuum level (Figure 4, Table 1).[13]

The UV—vis spectra of **3**—**6** show significant bathochromic shifts relative to that of the octyl-substituted monomer (**1d**) (Figure 5a), indicative of effective extension of π-conjugation for **3**—**6**. In contrast, **3**—**6** have similar absorption maxima (Figure 5a, Table 1), which implies that the extent of delocalization at their frontier orbitals is more or less similar to each other. Accordingly, the absorption edges also do not largely shift, indicating that the LUMO energy levels (E_{LUMO}) as well as the energy gap between the HOMO and LUMO (E_g) are not much influenced by the increase of the number of the BTT units (Table 1). On the other hand, the hyperchromic effect caused by the increased numbers of BTT units in the larger

oligomers is significant, and the molar extinction coefficient of the decamer (6) at 395 nm reaches to as high as 214,000 cm^{-1} M^{-1}. This observation and the lack of the size-dependent spectral shift suggest that the intramolecular electronic interaction between the BTT units is not so strong in the large oligomers.

Figure 5b shows their photo luminescence (PL) spectra in diluted solution. In contrast to the large Stokes shift observed for
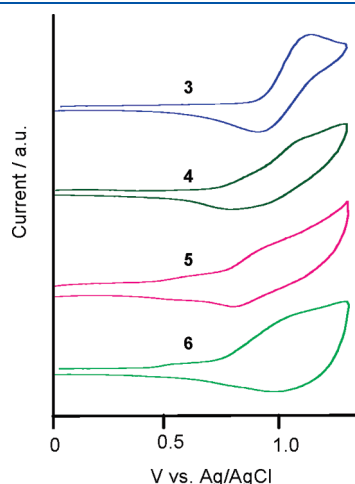
Figure 4. Cyclic voltammograms (scan rate 100 mV s^{-1}) of **3**−**6** recorded in benzonitrile (10^{-3} M) solution containing tetrabutylammonium hexafluorophosphate (Bu$_4$NPF$_6$, 10^{-1} M) as electrolyte with Pt working and counter electrodes.

1d (1.1 eV), the shifts of **3** (0.46 eV) and **4** (0.40 eV) are smaller, implying their rigid molecular structures with coplanarity in the excited state. The PL spectrum of **5** centered at ca. 550 nm is very weak and shifted bathochromically (Stokes shift 0.89 eV). This can be interpreted by considering the large and flexible molecular geometry of **5**, which can have access to different geometrical conformations and result in the bathochromically shifted spectrum. A similar red-shifted and very weak PL spectrum is also the case for **6**.

It is worth pointing out that the fluorescence quantum efficiencies of large dendritic oligomers (**5** and **6**) are very low (Table 1). Similar fluorescence quenching has been reported for a series of phenylacetylene- and oligothiophene-based dendrimers, and it has been interpreted by the consideration that the larger dendritic molecules may have many modes to dissipate the excitation energy, which enhances the nonradiative decay.[14] It is thus rational to conclude that **5** and **6** have considerable dendrimer-like nature, whereas **4** even with a dendritic structure is rather ordinary "small-molecule"-like.

Theoretical MO Calculation of BTT Dimer and Tetramer. In order to understand the experimental results on the molecular electronic properties, theoretical calculations with the DFT method at the B3LYP/6-31 g(d) level[15] were carried out for the parent BTT (**1a**), dimer (**2**), and the unsubstituted tetramer (Table S1 in Supporting Information). Different from the BTT monomer possessing the doubly degenerate frontier orbitals characteristic of the C_{3h} symmetric molecular structure (Figure S1 in Supporting Information), calculations of **2** indicated that nondegenerated HOMO (−5.28 eV below the vacuum level) and LUMO (−1.68 eV) with electron density delocalization over

Table 1. Experimental Data of Molecular Electronic Properties

	E^{ox}_{onset}, V^a	E_{HOMO},^{b} eV	E_g,^{c} eV	E_{LUMO},^{d} eV	λ_{max}, nm (ε)	λ_{edge}, nm	λ_{max} (PL), nm	Stokes shift, eV	ϕ_n
1d	+1.17	−5.5	3.9	−1.6	276 (72000)	316	370	1.1	e
3	+0.92	−5.3	2.9	−2.4	380 (32800)	433	450	0.46	0.083
4	+0.83	−5.2	2.7	−2.5	387 (95000)	456	450	0.40	0.055
5	+0.78	−5.1	2.6	−2.5	393 (144000)	475	547	0.89	e
6	+0.72	−5.0	2.5	−2.5	395 (214000)	498	545	0.87	e

^{a} Versus Ag/AgCl in benzonitrile containing Bu$_4$NPF$_6$ (10^{-1} M) as supporting electrolyte. The standard Fc/Fc$^+$ showed a redox couple at $E^{1/2}$ = +0.46 V under identical conditions. ^{b} Under the premise that the energy level of Fc/Fc$^+$ is 4.8 eV below the vacuum level, E_{HOMO}s were estimated from E^{ox}_{onset} (see ref 13). ^{c} Estimated from the absorption edge. ^{d} Calculated from the E_{HOMO} and E_g. ^{e} Very weak PL intensity was detected with ϕ_n less than 10^{-7}.
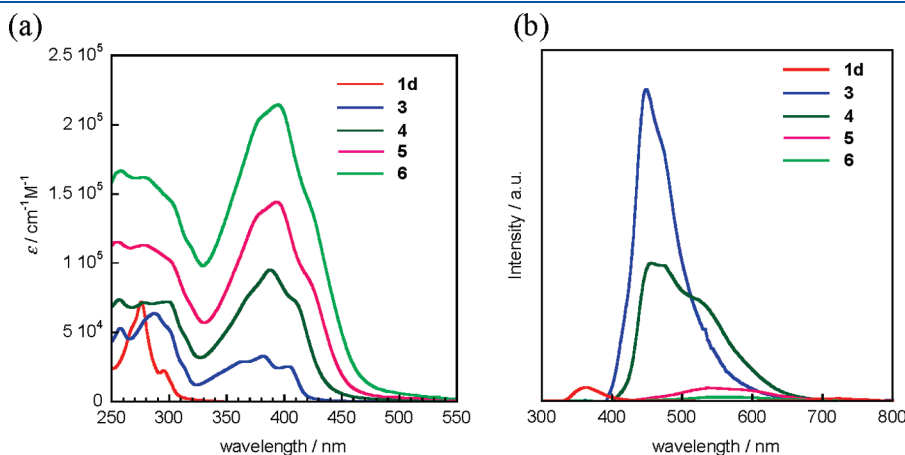
Figure 5. UV−vis (a) and PL (b) spectra of **1d** and **3**−**6**. Intensity of PL spectra is normalized with concentration and ε at the excitation wavelength (λ_{ex} 300 nm for **1d**, 380 nm for **3**, 387 nm for **4**, 393 nm for **5**, and 395 nm for **6**).
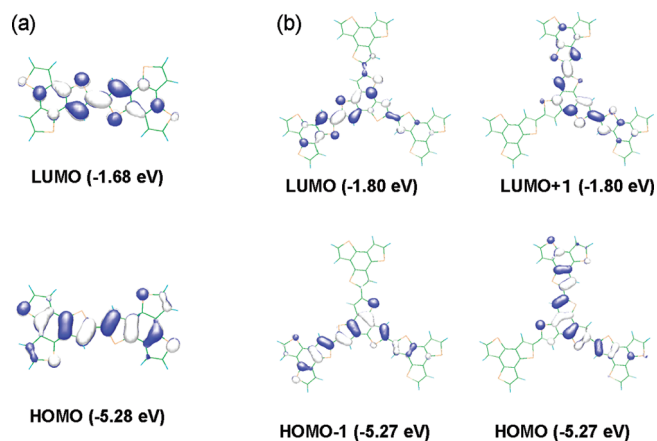
Figure 6. Non-degenerate HOMO and LUMO of BTT dimer (**2**) (a) and doubly degenerate HOMO and LUMO of BTT tetramer (b) calculated with the DFT method at the B3LYP/6-31 g(d) level.
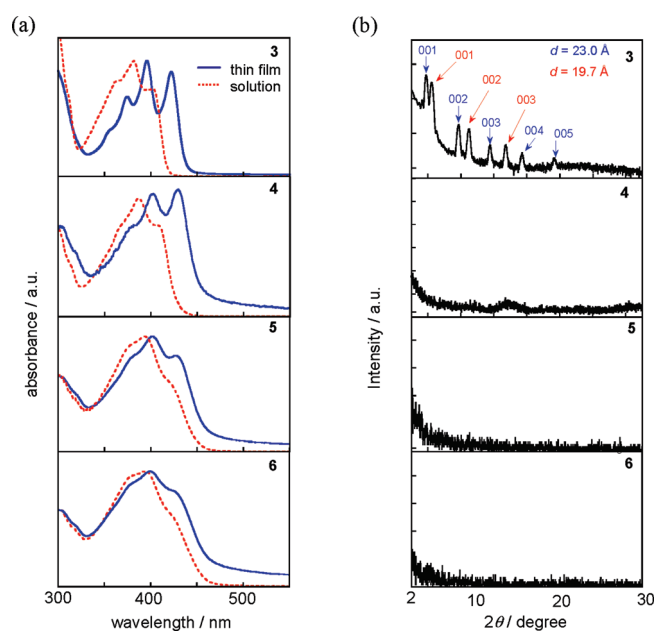
Figure 7. Absorption spectra (a) and XRD patterns of spin-coated thin films of **3**−**6** (b).

the whole molecule are characteristic (Figure 6a). In contrast, the dendritic tetramer, i.e., the core part of **4**, with C_{3h} symmetry, comes to have again doubly degenerated HOMO and LUMO (Figure 6b). It should be noted that the electron density is confined within two or three BTT parts in each orbital for the tetramer. Owing to the localized molecular orbitals, the energy levels of HOMO (−5.27 eV) and LUMO (−1.80 eV) are not very different from those of the dimer, well explaining the similar oxidation onsets in the cyclic voltammograms of **3** and **4** (Figure 4). Although the larger oligomers **5** and **6** are too large to carry out their MO calculations and hence the detailed pictures of their frontier orbitals are not clear, the extent of molecular orbital delocalization is expected to be similar to that of **4**.

Solution Deposited Thin Films of 3−6 and Their FET Devices. The physicochemical data as well as the theoretical calculations indicate that **3**−**6** have appropriate HOMO energy

levels for use as p-channel organic semiconductors. They are also soluble enough in common organic solvents for solution-deposition of their thin films. In fact, simple spin-coating method using the chloroform solution at room temperature gave their homogeneous thin films on quartz glass or Si/SiO₂ substrates. Depicted in Figure 7 are the absorption spectra and XRD patterns of the thin films of **3**−**6**. In absorption spectra, apparent red shifts (∼20 nm) are observed for the thin films of **3** and **4**, which is a strong indication of intermolecular π-overlap between the planar molecules in the thin film state as observed in the bulk single crystal structure of **3** (vide supra). On the other hand, larger oligomers (**5** and **6**) show smaller red shifts (less than 10 nm) than those for **3** and **4**, and in particular that for **6** is almost negligible. This observation can be well-understood by the nonplanar geometry of the large oligomers, especially **6**, with which it may be difficult to construct an intermolecularly interactive structure suitable for effective carrier transport.

As depicted in Figure 7b, only the thin film of **3** shows clear XRD peaks, indicating the formation of a crystalline thin film. As clearly seen from the multiple (00*l*) reflections, the film has a lamellar structure, although there exist two different molecular phases evidenced from two sets of (00*l*) reflections designated by the different colors (Figure 7b, top). Both series of XRD peaks, however, can not be indexed with the bulk single crystal cell, suggesting that the packing structure of **3** in the thin film is different from that in the bulk crystal phase. The calculated interlayer spacing (*d*-spacing) for the **3** thin film, 19.7 and 23.0 Å, was much shorter than the molecular length of **3** (ca. 30 Å), implying a large inclination of the molecular long axis from the substrate normal or edge-on orientation with the molecular short-axis standing on the substrate.

In sharp contrast, the thin film of **4** with the planar molecular geometry gives no peaks in the XRD, indicative of its amorphous nature (Figure 7b). Although the reasons for this are not clear, we speculate that its geometry with C_{3h} symmetry and six octyl groups reduce the crystallinity in the solid state. The larger oligomers (**5** and **6**) gave also amorphous films as anticipated from their nonplanar molecular structure.

In accordance with the molecular ordering in the thin film state, OFET devices fabricated with the thin films of **3** showed typical FET responses with moderately high field-effect mobility (μ_{FET}, 0.14 cm² V⁻¹ s⁻¹) and I_{on}/I_{off} of 10⁵ (Figure 8a, Table 2), which indicates that the BTT core is a useful building block for developing electronic materials. On the other hand, μ_{FET} values of **4**-based devices were lower by 2 orders of magnitude (1.4 × 10⁻³ cm² V⁻¹ s⁻¹, Figure 8b, Table 2). This can be rationalized by the amorphous nature of its thin film state. Even though the molecule itself has a planar geometry enabling intermolecularly interactive structure in the thin film state, long-range ordering, i.e., crystallinity, can be a key factor to enhance the mobility, which requires an effective and continuous intermolecular orbital overlap in the horizontal direction on the substrate.[16] Owing to the less interactive and amorphous nature of the thin films of **5** and **6**, their FET devices showed characteristics rather inferior to those of **3** and **4**, lower field-effect mobility (∼7 × 10⁻⁴ cm² V⁻¹ s⁻¹, Table 2) and smaller I_{on}/I_{off} ratio.

■ CONCLUSION

We have successfully synthesized BTT oligomers up to a dendritic decamer (**2**−**6**). Single crystal X-ray analysis of the
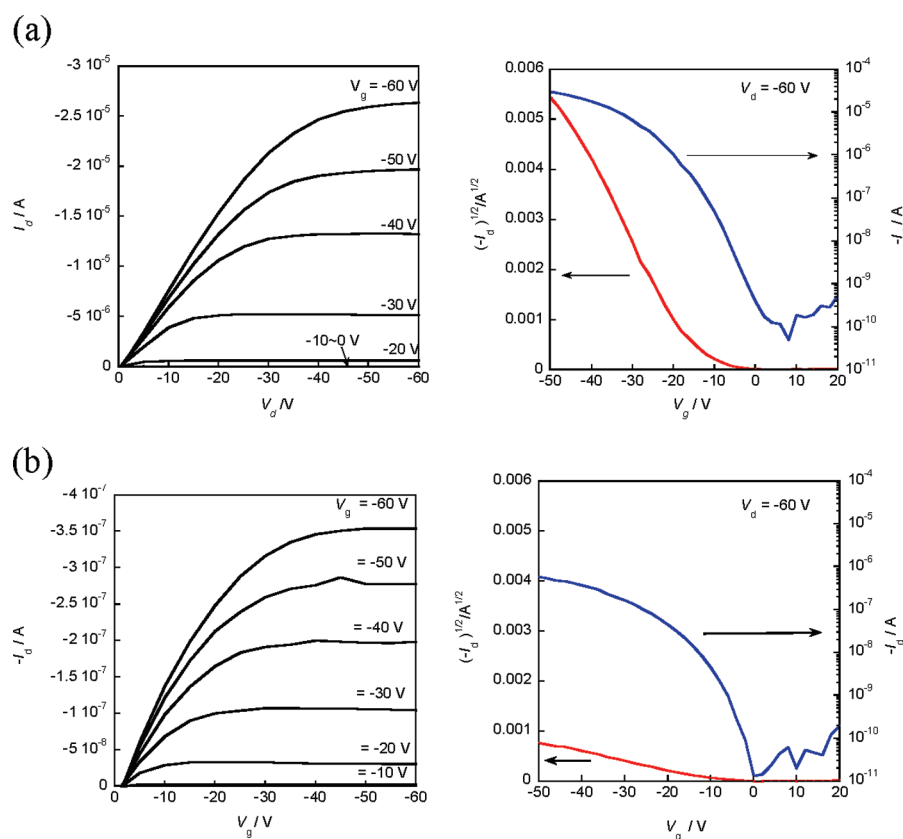
(a)

(b)

Figure 8. Output and transfer curves of **3**-based (a) and **4**-based OFETs (b).

Table 2. Thin Film Properties of 3−6

	$\Delta\lambda$, nm	d-spacing, Å	mobility, $cm^2\,V^{-1}\,s^{-1}$	I_{on}/I_{off}	V_{th}, V
3	14−20	19.7, 23.0	1.4×10^{-1}	10^5	−15
4	14−22	a	1.4×10^{-3}	10^4	−10
5	4−9	a	6×10^{-4}	10^4	−14
6	0−5	a	7×10^{-4}	10^4	−15

^{a} Amorphous film.

dimers (**2** and **3**) demonstrated that they both have good planarity and π-stacking crystal structures regardless of the presence/absence of the peripheral octyl groups, which indicates that BTT is a useful core unit that ensures coplanarity and an effective intermolecular π-stacking structure for developing new π-conjugated functional materials. Although the unsubstituted dimer (**2**) has poor solubility, alkylated oligomers (**3**−**6**) are soluble enough for the physicochemical characterizations and solution-deposition of their thin films. Evaluation of the oxidation potentials and solution absorption spectra, aided by the theoretical calculations, allow us to estimate the energy levels of their HOMO ($\sim$5.1 eV below the vacuum level) and HOMO−LUMO gaps, which suggests that their electronic structures are not strongly affected by the number of the BTT units in the molecule but by the extent of orbital delocalization over the BTT units. As a result, they are expected to be suitable as p-channel semiconductors rather than n-channel. In fact, solution deposited thin film of the dimer (**3**) with good molecular ordering in the thin film state acts as the active semiconducting layer in OFETs with μ_{FET} as high as 0.14 $cm^2\,V^{-1}\,s^{-1}$, whereas OFETs based on the larger oligomers gave rather lower mobility than that of **3**-based one, owing to the amorphous nature in the thin film state.

Although the FET mobilities of the higher oligomers are not very high, the present results on BTT oligomers indicate that the BTT core is a potential building block in developing new π-extended materials for opto/electronic applications. To do so, the control of morphology in the solid state is one of the key issues, and thus further modifications, including incorporation of other π-conjugated units and functional moieties, are now underway.

■ EXPERIMENTAL SECTION

Synthesis . All chemicals and solvents are of reagent grade unless otherwise indicated. Toluene and tetrahydrofuran (THF) were purified by standard distillation procedures prior to use. All reactions were carried out under nitrogen atmosphere unless otherwise stated. Benzo-[1,2-b:4,5-b':5,6-b'']trithiophene (**1a**) was synthesized according to reported procedures.[12] Melting points were uncorrected. Nuclear magnetic resonance spectra were, unless otherwise stated, obtained in deuterated chloroform with TMS as internal reference; chemical shifts (δ) are reported in parts per million. EI-MS spectra were obtained using an electron impact ionization procedure (70 eV). MALDI-TOF MS spectra were obtained using 1,8,9-trihydroxyanthracene matrix. The molecular ion peaks of sulfur, bromine or tin containing compounds showed a typical isotopic pattern, and all mass peaks are reported based on ^{32}S, ^{79}Br, or ^{120}Sn, respectively.

2,2'-Bi(benzo[1,2-b:3,4-b':5,6-b'']trithiophene) (2). **1a** (369 mg, 1.5 mmol) was dissolved in THF (18 mL). After the solution was cooled to 0 °C, a hexane solution of n-butyllithium (1.66 M, 1.08 mL,

1.8 mmol) was slowly added, and the resulting mixture was stirred at rt for 1.5 h. Fe(acac)$_3$ (349 mg, 0.98 mmol) was then added, and the resulting mixture was stirred at rt for 18h to give precipitates that was collected by filtration and washed successively with hydrochloric acid (2 M, 20 mL), water (20 mL), and ethanol (20 mL). The crude product was purified by vacuum sublimation (340 °C/10^{-3} Pa) to give **2** as yellow crystals (225 mg, 61%). Mp >300 °C; EI-MS m/z 490 (M$^+$). Anal. Calcd for C$_{24}$H$_{10}$S$_6$: C, 58.74; H, 2.05%. Found: C, 58.60; H, 1.98%.

2,5-Dioctylbenzo[1,2-*b*:3,4-*b'*:5,6-*b''*]trithiophene (7). **1a** (800 mg, 3.25 mmol) was placed in a test tube and dissolved in THF (80 mL). After the solution was cooled to 0 °C, a hexane solution of *n*-butyllithium (1.65 M, 4.64 mL, 7.24 mmol) was slowly added and then heated at 60 °C for 2 h. 1-Bromooctane (2.3 mL, 13 mmol) was then added, and stirring was continued at 60 °C for 12 h. After addition of saturated aqueous NH$_4$Cl solution (80 mL), the mixture was extracted with dichloromethane (10 mL × 2). The combined extract was washed with brine (80 mL × 3), dried over MgSO$_4$ (anhydrous), and concentrated in vacuo. The residue was subjected to flash column chromatography on silica gel eluted with hexane (R_f = 0.47, ϕ 2.5 × 5 cm). The product was further purified by preparative GPC (JAIGEL-1H/2H, CHCl$_3$, R_v = 184 mL) to give colorless crystals of 2,5-dioctylbenzo[1,2-*b*:3,4-*b'*:5,6-*b''*]trithiophene (**7**, 597 mg, 39%) together with 2,5,8-trioctylbenzo[1,2-*b*:3,4-*b'*:5,6-*b''*]trithiophene (**1d**, R_v = 205 mL, 411 mg, 29%). **7**: mp 36−38 °C; ^{1}H NMR (270 MHz) δ 7.53 (d, J = 5.3 Hz, 1H), 7.47 (d, J = 5.3 Hz, 1H), 7.27 (s, 1H), 7.22 (s, 1H), 2.98 (t, J = 7.6 Hz, 4H), 1.80 (quint, J = 7.6 Hz, 4H), 1.28−1.55 (m, 20H), 0.86−0.88 (m, 6H); ^{13}C NMR (99.5 MHz) δ 145.9, 145.8, 131.6, 131.5, 131.4, 130.5, 130.2, 129.9, 124.6, 122.3, 119.1, 119.0, 32.0(×2), 31.6(×2), 30.9(×2), 29.5(×2), 29.4(×2), 29.3(×2), 22.8(×2), 12.3(×2); EI-MS m/z = 470 (M$^+$). Anal. Calcd for C$_{28}$H$_{38}$S$_3$: C, 71.43; H, 8.14%. Found: C, 71.42; H, 8.34%. 2,5,8-Trioctylbenzo[1,2-*b*:3,4-*b'*:5,6-*b''*]trithiophene (**1d**): mp 41−43 °C; ^{1}H NMR (270 MHz, CDCl$_3$) δ 7.15 (s, 3H), 2.87 (t, J = 7.4 Hz, 4H), 1.72 (quint, J = 6.9 Hz, 4H), 1.24−1.28 (m, 30H), 0.87 (t, J = 6.6 Hz, 9H); ^{13}C NMR (99.5 MHz) δ 145.4, 131.4, 129.3, 118.9, 32.1, 31.6, 30.9, 29.6, 29.5, 29.3, 22.9, 14.3; EI-MS m/z = 582 (M$^+$). Anal. Calcd for C$_{36}$H$_{54}$S$_3$: C, 74.16; H, 9.34%. Found: C, 74.09; H, 9.45%.

2,2′-Bi(5,8-dioctylbenzo[1,2-*b*:3,4-*b'*:5,6-*b''*]trithiophene) (3). **7** (100 mg, 0.21 mmol) was dissolved in THF (2.5 mL). After the solution was cooled to 0 °C, a hexane solution of *n*-butyllithium (1.59 M, 0.20 mL, 0.32 mmol) was slowly added, and the resulting mixture was stirred at 60 °C for 1.5 h. Fe(acac)$_3$ (111 mg, 0.32 mmol) was then added, and the mixture was stirred at the same temperature for 20 h. The mixture was then diluted with saturated ammonium chloride aqueous solution (5 mL), and extracted with chloroform (20 mL × 2). The combined extract was washed with brine (50 mL × 3), dried over MgSO$_4$ (anhydrous), and concentrated in vacuo. Column chromatography on silica gel (ϕ 3 × 8 cm) eluted first with hexane and then hexane-dichloromethane (v/v = 3:1, R_f = 0.5) gave **3** (90 mg, 90%) as a pale yellow solid. The product was further purified by GPC followed by recrystallization from hexane for the device preparation. Mp 158−160 °C; ^{1}H NMR (400 MHz) δ 7.64 (s, 2H), 7.19 (s, 2H), 7.17 (s, 1H), 2.97 (t, J = 7.0 Hz, 8H), 1.81 (quint, J = 7.0 Hz, 8H), 1.32 (m, 16H), 0.89 (t, J = 7.0 Hz, 12H); ^{13}C NMR (99.5 MHz) δ 146.2, 146.1, 136.0, 132.0, 131.9, 131.2, 130.7, 129.9, 129.6, 119.1, 119.0, 118.9, 32.0(×2), 31.6(×2), 30.9(×2), 30.0(×2), 29.4(×2), 29.3(×2), 22.8(×2), 14.3(×2); MALDI-TOF MS m/z = 939.70 (M$^+$). Anal. Calcd for C$_{56}$H$_{74}$S$_6$: C, 71.58; H, 7.94%. Found: C, 71.40; H, 7.93%.

(5,8-Dioctylbenzo[1,2-*b*:3,4-*b'*:5,6-*b''*]trithiophen-2-yl)trimethylstannane (8). **7** (600 mg, 1.27 mmol) was placed in a 100 mL round-bottomed flask and dissolved in THF (40 mL). After the solution was cooled to 0 °C, a hexane solution of *n*-butyllithium (1.57 M, 2.0 mL, 3.14 mmol) was slowly added, and the resulting mixture was stirred at rt for 1.5 h. Trimethyltin chloride (586 mg, 3.14 mmol) was then added,

and stirring was continued for 1.5 h. After addition of saturated NH$_4$Cl aqueous solution (20 mL), the mixture was extracted with dichloromethane (10 mL × 2). The combined extract was washed with brine (20 mL × 3), dried over MgSO$_4$ (anhydrous), and concentrated in vacuo. The resulting residue was subjected to flash column chromatography on alumina eluted with hexane. The product was further purified by GPC (JAIGEL-1H/2H, CHCl$_3$, R_v = 148 mL) to give **8** (707 mg, 88%) as a white solid. Mp 41−43 °C; ^{1}H NMR (400 MHz) δ 7.58 (s, 1H), 7.27 (s, 1H), 7.21 (s, 1H), 2.95−2.99 (m, 4H), 1.77−1.83 (m, 4H), 1.55−1.28 (m, 20H), 0.86−0.96 (m, 6H), 0.46 (s, $^3J_{Sn-H}$ = 28.6 Hz, 9H); ^{13}C NMR (99.5 MHz) δ 145.5, 145.4, 138.0, 135.3, 132.9, 131.3, 131.2, 129.9, 129.5, 129.2, 119.3, 118.8, 31.9(×2), 31.4(×2), 30.7(×2), 29.3(×2), 29.2(×2), 29.13(×2), 22.7(×2), 14.1(×2), −8.2; EI-MS m/z = 634 (M$^+$). Anal. Calcd for C$_{31}$H$_{46}$S$_3$Sn: C, 58.76; H, 7.32%. Found: C, 59.03; H, 7.35%.

2,5,8-Tribromobenzo[1,2-*b*:3,4-*b'*:5,6-*b''*]trithiophene (9). To a well-stirred solution of **1a** (800 mg, 3.25 mmol) in dichloromethane (22.7 mL) and acetic acid (5.7 mL) in a 50 mL round bottom flask under nitrogen atmosphere was slowly added *N*-bromosuccinimide (1.74 g, 9.74 mmol) in small portions. The resulting mixture was stirred at room temperature for 60 h, and then added water (10 mL) was added to precipitate the product. The precipitate was collected by filtration, washed with water (10 mL × 2) and ethanol (4 mL × 2), and dried in vacuo. Recrystallization from chlorobenzene gave **9** as pale violet needles (1.22 g, 77%). Mp 230 °C; ^{1}H NMR (270 MHz) δ 7.50 (s, 3H); EI-MS m/z = 480 (M$^+$). Anal. Calcd for C$_{12}$H$_3$S$_3$Br$_3$: C, 29.84; H, 0.63%. Found: C, 30.05; H, 0.67%.

2′,5′,8′-Tris(5,8-dioctylbenzo[1,2-*b*:3,4-*b'*:5,6-*b''*]trithiophen-2-yl)benzo[1,2-*b*:3,4-*b'*:5,6-*b''*]trithiophene (4). **8** (210 mg, 0.33 mmol) and **9** (44 mg, 0.091 mmol) were placed in a two-necked flask with a reflux condenser and dissolved in DMF (7 mL). The solution was deaerated by nitrogen stream, then Pd(PPh$_3$)$_4$ (36 mg, 31 μmol) was added, and the resulting mixture was refluxed for 12 h. After cooling, the mixture was diluted with water (5 mL) to precipitate the product. The precipitate was collected by filtration, washed with water (5 mL × 2) and ethanol (5 mL × 2), and dried in vacuo to give crude **4** as a yellow solid. The solid was subjected to column chromatography on silica gel (R_f = 0.50, hexane/CS$_2$, 1:1, v/v, ϕ 5 × 10 cm) and further purified by recrystallization from CHCl$_3$/ethanol (1:1, v/v) to give analytically pure **4** (121 mg, 81%) as a yellow solid. Mp 223−225 °C; ^{1}H NMR (400 MHz) δ 7.17 (s, 3H), 7.01 (s, 3H), 6.75 (s, 3H), 6.68 (s, 3H), 2.75 (m, 12H), 1.71 (m, 12H), 1.34 (m, 60H), 0.94 (t, J = 6.3 Hz, 18H); MALDI-TOF MS m/z = 1651.81 (M$^+$). Anal. Calcd for C$_{96}$H$_{114}$S$_{12}$: C, 69.77; H, 6.95%. Found: C, 69.50; H, 6.72%.

8′-Bromo-5,5′′,8,8′′-tetraoctyl-2,2′:5′,2′′-terbenzo[1,2-*b*:3,4-*b'*:5,6-*b''*]trithiophene (10). **8** (222 mg, 350 μmol) and **9** (94 mg, 195 μmol) were placed in a test tube with a reflux condenser and dissolved in DMF (5 mL). To the deaerated solution was added Pd(PPh$_3$)$_4$ (16 mg, 14 μmol). The resulting mixture was heated at 80 °C for 12 h and, after cooling, diluted with water (5 mL) to precipitate the product. The product was collected by filtration, washed with water (5 mL × 2) and ethanol (5 mL × 2), and dried in vacuo to give crude **10** as a yellow solid. The crude **10** was subjected to flash column chromatography on alumina eluted with dichloromethane and further purified by preparative GPC (JAIGEL-1H/2H, CHCl$_3$) to give **10** as a yellow solid (94 mg, 42%). Mp 111−113 °C; ^{1}H NMR (400 MHz) δ 7.00 (s, 1H), 6.92 (s, 1H), 6.88 (s, 1H), 6.83 (s, 1H), 6.77 (s, 1H), 6.71 (s, 1H), 6.68 (s, 1H), 6.67 (s, 1H), 6.63 (s, 1H), 2.75−2.67 (m, 8H), 1.66−1.62 (m, 8H), 1.38−1.26 (m, 40H), 0.92 (t, J = 6.4 Hz, 12H); ^{13}C NMR (126 MHz) δ 145.7(×2), 145.5(×2), 136.7(×2), 135.1, 135.0, 131.8(×2), 131.6(×2), 131.2(×4), 130.7(×2), 130.6(×2), 130.4(×2), 129.4(×2), 129.1(×2), 124.5, 118.5(×2), 118.3(×3), 118.2(×3), 113.6, 31.9 (×4), 31.2 (×2), 31.1 (×2), 30.8 (×3), 30.7, 29.5 (×4), 29.4 (×8), 22.8 (×4), 14.1(×4); MALDI-TOF MS m/z 1263 (M$^+$). Anal. Calcd for C$_{68}$H$_{77}$BrS$_9$: C, 64.67; H, 6.15%. Found: C, 64.72; H, 6.04%.

2,5,8-Tris(trimethylstannyl)benzo[1,2-b:3,4-b′:5,6-b″]tri-thiophene (11). Benzo[1,2-b:4,5-b′:5,6-b″]trithiophene (**1a**, 1.0 g, 4.06 mmol) was placed in a 50-mL round-bottomed flask and dissolved in THF (50 mL). After the solution was cooled at 0 °C, a hexane solution of n-butyllithium (1.59 M, 15.3 mL, 24.4 mmol) was slowly added and then stirred at room temperature for 6 h. Trimethyltin chloride (2.67 g, 13.4 mmol) was then added, and the mixture was stirred at rt overnight. After addition of water (20 mL), the mixture was extracted with dichloromethane (50 mL × 3). The combined extracts were washed with water (50 mL × 3), dried over MgSO₄ (anhydrous), and concentrated in vacuo. The product was purified by recrystallization from hexane/methanol to give **11** (3.0 g, quantitative) as a white solid. Mp 212−213 °C; ^{1}H NMR (400 MHz) δ 7.69 (s with satellite peaks, $^3J_{Sn-H}$ = 14 Hz, 3H), 0.476 (s with satellite peaks, $^3J_{Sn-H}$ = 41.2 Hz, 27H); ^{13}C NMR (99.5 MHz) δ 138.0, 135.8, 132.7, 130.4, −8.15. Anal. Calcd for $C_{21}H_{30}S_3Sn_3$: C, 34.33; H, 4.12%. Found: C, 34.59; H, 3.75%.

2,5-Dioctyl-8-iodobenzo[1,2-b:3,4-b′:5,6-b″]trithiophene (12). **7** (940 mg, 2.0 mmol) was placed in a 50 mL round-bottomed flask and dissolved in THF (28 mL). After the solution was cooled to 0 °C, a hexane solution of n-butyllithium (1.57 M, 1.6 mL, 2.5 mmol) was slowly added, and the mixture was stirred at rt for 1.5 h. Then a solution of iodine (660 mg, 2.6 mmol) in THF (28 mL) was added dropwise, and the resulting mixture was stirred for 1.5 h. After addition of an aqueous NaHSO₃ solution (10 mL), the mixture was extracted with dichloromethane (20 mL × 2). The extract was washed with an aqueous NaHSO₃ solution (20 mL × 3), dried over MgSO₄ (anhydrous), and concentrated in vacuo. The residue was purified by column chromatography on silica gel (R_f = 0.6, hexane, ϕ 3.5 × 14 cm) to give **12** (920 mg, 78%) as a white solid. Mp 53−55 °C; ^{1}H NMR (400 MHz) δ 7.70 (s, 1H), 7.19 (s, 1H), 7.16 (s, 1H), 2.96 (t, J = 8.0 Hz, 4H), 1.77 (m, 4H), 1.28−1.42 (m, 40H), 0.88 (t, J = 6.3 Hz, 6H); ^{13}C NMR (99.5 MHz) δ 146.3, 146.2, 135.1, 132.4, 132.0(×2), 131.7, 130.4, 128.2, 118.7(×2), 74.9, 31.9(×2), 31.4(×2), 30.7(×2), 29.3(×2), 29.2(×2), 29.1(×2), 22.7(×2), 14.1(×2); EI-MS m/z 550 (M⁺). Anal. Calcd for $C_{28}H_{37}IS_3$: C, 56.36; H, 6.25%. Found: C, 56.36; H, 6.25%.

Trimethyl(5,5″,8,8″-tetraoctyl-[2,2′:5′,2″-terbenzo[1,2-b:3,4-b′:5,6-b″]trithiophen]-8′-yl)stannane (13). **12** (282 mg, 473 μmol) and **11** (194 mg, 264 μmol) were placed in a 20 mL-round-bottomed flask, and dissolved in DMF (9.4 mL). To the deaerated solution was added Pd(PPh₃)₄ (30 mg, 12 μmol). The resulting mixture was heated at 80 °C for 12 h, cooled to rt, and then added water (5 mL) to precipitate the product. The precipitate was collected by filtration, washed with water (5 mL × 2) and ethanol (5 mL × 2), and dried in vacuo to give crude product as a yellow solid. The crude product was subjected to flash column chromatography on alumina eluted with dichloromethane, and then further purified by preparative GPC (JAIGEL-1H/2H, CHCl₃) to give **13** as a yellow solid (265 mg, 83%). ^{1}H NMR (400 MHz) δ 7.75 (s, 1H), 7.73 (s, 1H), 7.71 (s, 1H), 7.69 (s, 1H), 7.64 (s, 1H), 7.23 (s, 2H), 7.20 (s, 1H), 7.18 (s, 1H), 3.01−2.96 (m, 8H), 1.84−1.82 (m, 8H), 1.51−1.31 (m, 40H), 0.90 (t, J = 6.4 Hz, 12H), 0.53 (s, $^3J_{Sn-H}$ = 28.6 Hz, 9H); ^{13}C NMR (126 MHz) δ 145.8(×2), 145.7(×2), 138.9(×2), 136.7, 136.3(×2), 135.6, 135.5, 133.0, 132.0, 131.9, 131.8, 131.7, 131.6, 131.2, 131.0(×2), 130.8, 130.5(×2), 130.0, 129.8, 129.7(×2), 129.5, 129.4, 118.8, 118.7(×3), 118.6(×3), 118.3, 32.0 (×4), 31.4 (×3), 31.4, 30.8 (×3), 30.7, 29.5 (×4), 29.4 (×4), 29.3 (×4), 22.7 (×4), 14.1(×4), −8.0(×4); MALDI-TOF MS m/z 1263 (M⁺). Anal. Calcd for $C_{71}H_{86}S_9Sn$: C, 63.32; H, 6.44%. Found: C, 63.27; H, 6.24%.

2,2′-Bis{5,8-bis(5″,8″-dioctylbenzo[1,2-b:3,4-b′:5,6-b″]-trithiophen-2″-yl)}benzo[1,2-b:3,4-b′:5,6-b″]trithiophene (5). **13** (53 mg, 40 μmol) and **10** (50 mg, 40 μmol) were placed in a test tube and dissolved in toluene (1 mL). To the deaerated solution was added Pd(PPh₃)₄ (3 mg, 2.4 μmol). The resulting mixture was refluxed for 16 h, cooled to rt, diluted with water (1 mL), and extracted with dichloromethane (10 mL × 2). The combined extracts were washed with brine (20 mL × 3) and dried over MgSO₄ (anhydrous).

Evaporation of the solvent gave a crude product. Then the product was subjected to flash column chromatography on alumina eluted with dichloromethane and further purified by preparative GPC (JAIGEL-1H/2H, CHCl₃) to give **5** (55 mg, 67%). Mp >300 °C; ^{1}H NMR (400 MHz, CD₂Cl₂, 100 °C) δ 7.2−6.2 (broad peaks, 18H), 2.7 (broad peaks, 16H), 1.7−0.9 (broad peaks, 120H); MALDI-TOF MS m/z 2365 (M⁺). Anal. Calcd for $C_{136}H_{154}S_{18}$: C, 69.04; H, 6.56%. Found: C, 68.96; H, 6.54%.

2,5,8-Tris{(5′,8′-bis(5″,8″-dioctylbenzo[1,2-b:3,4-b′:5,6-b″]trithiophen-2″-yl)benzo[1,2-b:3,4-b′:5,6-b″]trithiophen-2′-yl)}benzo[1,2-b:3,4-b′:5,6-b″]trithiophene (6). **9** (20 mg, 41 μmol) and **13** (200 mg, 148 μmol) were placed in a test tube with a reflux condenser, and dissolved in toluene (2 mL). To the deaerated solution was added Pd(PPh₃)₄ (5 mg, 4 μmol). The resulting mixture was refluxed for 16 h, cooled to rt, diluted with water (1 mL), and extracted with dichloromethane (10 mL × 2). The extract was washed with brine (20 mL × 3) and dried over MgSO₄ (anhydrous). Evaporation of the solvent gave a crude product, which was subjected to flash column chromatography on alumina eluted with dichloromethane. The product was further purified by preparative GPC (JAIGEL-1H/2H, CHCl₃) to give mixture of **6** and **5** as a brown solid. The mixture was again purified by preparative GPC (JAIGEL-2H/3H, CHCl₃) to give **6** as a brown solid (51 mg, 33%). Mp >300 °C; MALDI-TOF MS m/z 3792 (M⁺). Anal. Calcd for $C_{216}H_{234}S_{30}$: C, 68.41; H, 6.22%. Found: C, 68.13; H, 6.03%.

*X-ray Crystallographic Analysis of **2** and **3**.* Single crystals suitable for structural analysis were obtained by careful recrystallization from chloroform. The X-ray crystal structure analysis was made on a Rigaku RAXIS-RAPID Imaging Plate (Mo Kα radiation, λ = 0.71069 Å, graphite monochromator, T = 200 K, $2\theta_{max}$ = 55.0°). The structure was solved by the direct methods.[17] Non-hydrogen atoms were refined anisotropically, and hydrogen atoms were included in the calculations but not refined. All calculations were performed using the crystallographic software SHELX-97.[17] In the structure of **2**, orientationally disordered molecules related by the C_2 axis on the molecular long axis exist. Thus, the population of the sulfur and α-carbon atoms suggested that ca. 32% molecules were disordered.

Crystal data for **2**: $C_{24}H_{10}S_6$, M = 490.70, yellow needle, 0.80 × 0.10 × 0.10 mm³, monoclinic, space group, $P2_1/n$ (No. 14), a = 16.683(18), b = 8.90(4), c = 17.88(19) Å, β = 115.15(3)°, V = 1009.7(19) Å³, Z = 2, R = 0.0966, wR^2 = 0.1393 for all observed reflections (2099) and 191 variable parameters.

Crystal data for **3**: $C_{56}H_{74}S_6$, M = 939.56, yellow needle, 0.50 × 0.30 × 0.050 mm³, triclinic, space group, P-1 (No. 2), a = 10.255(5), b = 15.864(7), c = 17.626(8) Å, α = 66.05(1), β = 84.59(2), γ = 89.06(2) °, V = 2608(2) Å³, Z = 2, R = 0.0622, wR^2 = 0.2286 for all observed reflections (6222) and 559 variable parameters.

Device Fabrications and Evaluations. OFETs. Si/SiO₂ substrates were treated with octyltrichlorosilane (OTS-8) by immersing the silicon wafers to OTS-8 solution in dry toluene at room temperature under nitrogen for 12 h.[18] OFETs were fabricated in a "top-contact" configuration on a heavily doped n^+-Si (100) wafer with 200-nm-thick thermally grown SiO₂ (C_i = 17.3 nF cm^{-2}). A thin film of **3** or **4** as the active layer was spin-coated on Si/SiO₂ substrates at 3000 rpm for 30 s. On top of the organic thin film, gold films (80 nm) as drain and source electrodes were deposited through a shadow mask. For a typical device, the drain-source channel length (L) and width (W) are 50 μm and ca. 1.5 mm, respectively. The characteristics of the OFET devices were measured at room temperature in air with a Keithly 4200 semiconducting parameter analyzer. Field-effect mobility (μ_{FET}) was calculated in the saturation regime (V_d = −60 V) of the I_d using the following equation:

$$I_d = (WC_i/2L)\mu_{FET}(V_g - V_{th})^2$$

where C_i is the capacitance of the SiO₂ insulator, and V_g and V_{th} are the gate and threshold voltages, respectively. Current on/off ratio (I_{on}/I_{off})

was determined from the I_d at $V_g = 0$ V (I_{off}) and $V_g = -60$ V (I_{on}). The μ_{FET} data reported in the present paper are values from more than 10 different devices.

■ ASSOCIATED CONTENT

ⓢ Supporting Information. Crystallographic information files (CIF format) for **2** and **3**, complete ref 15, FET characteristics of **5**- and **6**-based OFETs, results of MO calculations, and AFM images of thin films, NMR spectra, MALDI-TOF MS spectra of **5** and **6**. This material is available free of charge via the Internet at http://pubs.acs.org.

■ AUTHOR INFORMATION

Corresponding Author
*E-mail: ktakimi@hiroshima-u.ac.jp.

■ ACKNOWLEDGMENT

■ REFERENCES

(1) (a) *Organic Electronics, Manufacturing and Applications*; Klauk, H., Ed.; Wiley-VCH: Weinheim, 2006. (b) *Electronic Materials: The Oligomer Approache*; Müllen, K., Wegner, G., Ed.; Wiley-VCH: Weinheim, 1998. (c) See also a special issue on π-functional materials: Bredas, J.-L.; Marder, S. R.; Reichmanis, E. *Chem. Mater.* **2011**, *23*, 309–922.

(2) (a) Gundlach, D. J.; Lin, Y. Y.; Jackson, T. N.; Nelson, S. F.; Schlom, D. G. *IEEE Electron Device Lett.* **1997**, *18*, 87–89. (b) Anthony, J. E. *Chem. Rev.* **2006**, *106*, 5028–5048. (c) Anthony, J. E. *Angew. Chem., Int. Ed.* **2008**, *47*, 452–483.

(3) (a) McCullough, R. D.; Lowe, R. D. *J. Chem. Soc., Chem. Commun.* **1992**, 70–72. (b) Chen, T.; Rieke, R. D. *J. Am. Chem. Soc.* **1992**, *114*, 10087–10088. (c) Roncali, J. *Chem. Rev.* **1992**, *92*, 711–738. (d) McCullough, R. D. *Adv. Mater.* **1998**, *10*, 93–116. (e) Bao, Z.; Dodabalapur, A.; Lovinger, A. J. *Appl. Phys. Lett.* **1996**, *69*, 4108–4110. (f) Sirringhaus, H.; Brown, P. J.; Friend, R. H.; Nielsen, M. M.; Bechgaard, K.; Langeveld-Voss, B. M. W.; Spiering, A. J. H.; Janssen, R. A. J.; Meijer, E. W.; Herwig, P.; De Leeuw, D. M. *Nature* **1999**, *401*, 685–688. (g) Perepichka, I. F.; Perepichka, D. F.; Meng, H.; Wudl, F. *Adv. Mater.* **2005**, *17*, 2281–2305.(h) Jeffries-El, M.; McCullough, R. D. In *Handbook of Conducting Polymers*, 3rd ed.; Skotheim, T. A.; Reynolds, J. R., Eds; CRC Press: Boca Raton, FL, 2007; Vol. 1, Chapter 9. (i) Ewbank, P. C.; Laird, D.; McCullough, R. D. In *Organic Photovoltaics*; Brabec, C., Dyakonov, V., Scherf, U., Eds; Wiley-VCH: Weinheim, 2008, Chapter 1. (j) Fichou, D.; Zieglar, C. *Handbook of Oligo- and Polythiophenes*; Fichou, D., Ed.; Wiley-VCH: Weinheim, 1999.

(4) (a) Mckeown, N. B. *Phthalocyanine Materials: Synthesis, Structure and Function*; Cambridge University Press: Cambridge, MA, 1998. (b) Tang, C. W. *Appl. Phys. Lett.* **1986**, *48*, 183–185. (c) VanSlyke, S. A.; Chen, C. H.; Tang, C. W. *Appl. Phys. Lett.* **1996**, *69*, 2160–2162. (d) Bao, Z.; Lovinger, A. J.; Dodavalapur, A. *Appl. Phys. Lett.* **1996**, *69*, 3066–3068. (e) Bao, Z.; Lovinger, A. J.; Brown, J. *J. Am. Chem. Soc.* **1998**, *120*, 207–208. (f) Xue, J. G.; Uchida, S.; Rand, B. P.; Forrest, S. R. *Appl. Phys. Lett.* **2004**, *85*, 5757–5759.

(5) (a) Simpson, C. D.; Wu, J.; Watson, M. D.; Müllen, K. *J. Mater. Chem.* **2004**, *14*, 494–504. (b) Wu, J.; Pisula, W.; Müllen, K. *Chem. Rev.* **2007**, *107*, 718–747. (c) Feng, X.; Marcon, V.; Pisula, W.; Hansen,

M. R.; Kirkpatrick, J.; Grozema, F.; Andrienko, D.; Kremer, K.; Müllen, K. *Nat. Mater.* **2009**, *8*, 421–426.

(6) Several heteroarene-based p-OFETs showing μ_{FET} higher than 1.0 cm^2 V^{-1} s^{-1} have been reported: (a) Payne, M. M.; Parkin, S. R.; Anthony, J. E.; Kuo, C. C.; Jackson, T. N. *J. Am. Chem. Soc.* **2005**, *127*, 4986–4987. (b) Takimiya, K.; Ebata, H.; Sakamoto, K.; Izawa, T.; Otsubo, T.; Kunugi, Y. *J. Am. Chem. Soc.* **2006**, *128*, 12604–12605. (c) Yamamoto, T.; Takimiya, K. *J. Am. Chem. Soc.* **2007**, *129*, 2224–2225. (d) Ebata, H.; Izawa, T.; Miyazaki, E.; Takimiya, K.; Ikeda, M.; Kuwabara, H.; Yui, T. *J. Am. Chem. Soc.* **2007**, *129*, 15732–15733. (e) Gao, P.; Beckmann, D.; Tsao, H. N.; Feng, X.; Enkelmann, V.; Baumgarten, M.; Pisula, W.; Müllen, K. *Adv. Mater.* **2009**, *21*, 213–216. (f) Kang, M. J.; Doi, I.; Mori, H.; Miyazaki, E.; Takimiya, K.; Ikeda, M.; Kuwabara, H. *Adv. Mater.* **2011**, *23*, 1222–1225. (g) Shinamura, S.; Osaka, I.; Miyazaki, E.; Nakao, A.; Yamagishi, M.; Takeya, J.; Takimiya, K. *J. Am. Chem. Soc.* **2011**, *133*, 5224–5035.

(7) (a) Proetzsch, R.; Bieniek, D.; Korte, F. *Tetrahedron Lett.* **1972**, *13*, 543–544. (b) Jayasuriya, N.; Kagan, J.; Owens, J. E.; Kornak, E. P.; Perrine, D. M. *J. Org. Chem.* **1989**, *54*, 4203–4205.

(8) (a) Grayson, S. M.; Frechet, J. M. J. *Chem. Rev.* **2001**, *101*, 3819–3868. (b) Negishi, N.; Ie, Y.; Taniguchi, M.; Kawai, T.; Tada, H.; Kaneda, T.; Aso, Y. *Org. Lett.* **2007**, *9*, 829–832. (c) Wong, K.-T.; Lin, Y.-H.; Wu, H.-H.; Fungo, F. *Org. Lett.* **2007**, *9*, 4531–4534. (d) Jiang, Y.; Lu, Y.-X.; Cui, Y.-X.; Zhou, Q.-F.; Ma, Y.; Pei, J. *Org. Lett.* **2007**, *9*, 4539–4542. (e) Ma, C.-Q.; Fonrodona, M.; Schikora, M. C.; Wienk, M. M.; Janssen, R. A. J.; Bäuerle, P. *Adv. Funct. Mater.* **2008**, *18*, 3323–3331. (f) Lo, S.-C.; Burn, P. L. *Chem. Rev.* **2007**, *107*, 1097–1116. (g) Roncali, J.; Leriche, P.; Cravino, A. *Adv. Mater.* **2007**, *19*, 2045–2060. (h) Kanibolotsky, A. L.; Perepichka, I. F.; Skabara, P. J. *Chem. Soc. Rev.* **2010**, *39*, 2695–2728.

(9) (a) Bettignies, R. d.; Nicolas, Y.; Blanchard, P.; Levillain, E.; Nunzi, J. M.; Roncali, J. *Adv. Mater.* **2003**, *15*, 1939–1943. (b) Nicolas, Y.; Blanchard, P.; Levillain, E.; Allain, M.; Mercier, N.; Roncali, J. *Org. Lett.* **2004**, *6*, 273–276. (c) Piot, L.; Silly, F.; Tortech, L.; Nicolas, Y.; Blanchard, P.; Roncali, J.; Fichou, D. *J. Am. Chem. Soc.* **2009**, *131*, 12864–12865.

(10) Taerum, T.; Lukoyanova, O.; Wylie, R. G.; Perepichka, D. F. *Org. Lett.* **2009**, *11*, 3230–3233.

(11) Demenev, A.; Eichhorn, S. H.; Taerum, T.; Perepichka, D. F.; Patwardhan, S.; Grozema, F. C.; Siebbeles, L. D. A.; Klenkler, R. *Chem. Mater.* **2010**, *22*, 1420–1428.

(12) Kashiki, T.; Shinamura, S.; Kohara, M.; Miyazaki, E.; Takimiya, K.; Ikeda, M.; Kuwabara, H. *Org. Lett.* **2009**, *11*, 2473–2475.

(13) (a) Pommerehne, J.; Vestweber, H.; Guss, W.; Mahrt, R. F.; Bässler, H.; Porsch, M.; Daub, J. *Adv. Mater.* **1995**, *7*, 551–554. (b) Johansson, T.; Mammo, W.; Svensson, M.; Andersson, M. R.; Inganas, O. *J. Mater. Chem.* **2003**, *13*, 1316–1323.

(14) (a) Devadoss, C.; Bharathi, P.; Moore, J. S. *J. Am. Chem. Soc.* **1996**, *118*, 9635–9644. (b) Devadoss, C.; Bharathi, P.; Moore, J. S. *Macromolecules* **1998**, *31*, 8091–8099. (c) Ramakrishna, G.; Bhaskar, A.; Bäuerle, P.; Goodson, T. *J. Phys. Chem. A* **2007**, *112*, 2018–2026. (d) Badaeva, E.; Harpham, M. R.; Guda, R.; Süzer, O.; Ma, C.-Q.; Bäuerle, P.; Goodson, T.; Tretiak, S. *J. Phys. Chem. B* **2010**, *114*, 15808–15817.

(15) MO calculations were carried out with the DFT method at the B3LYP/6-31g(d) level using Gaussian 03 program package. Frisch, M. J. *Gaussian 03, revision C.02*; Gaussian, Inc.: Wallingford, CT, 2004.

(16) Dimitrakopoulos, C. D.; Malenfant, P. R. L. *Adv. Mater.* **2002**, *14*, 99–117.

(17) Sheldrick, G. M. *SHELXL (SHELX97) Programs for the Refinement of Crystal Structures*; University of Goettingen: Germany, 1997.

(18) Ong, B. S.; Wu, Y.; Liu, P.; Gardner, S. *J. Am. Chem. Soc.* **2004**, *126*, 3378–3379.